Clinical implications of subclonal *TP53* mutations in acute myeloid leukemia

Katharina T. Prochazka,[1]* Gudrun Pregartner,[2]* Frank G. Rücker,[3] Ellen Heitzer,[4] Gabriel Pabst,[1] Albert Wölfler,[1] Armin Zebisch,[1] Andrea Berghold,[2] Konstanze Döhner[3] and Heinz Sill[1]****

[1]Division of Hematology, Medical University of Graz, Austria; [2]Institute for Medical Informatics, Statistics and Documentation, Medical University of Graz, Austria; [3]Department of Internal Medicine III, University Hospital of Ulm, Germany and [4]Institute of Human Genetics, Medical University of Graz, Austria

**KTP and GP contributed equally to this work.*

***KD and HS contributed equally to this work.*

 doi:10.3324/haematol.2018.205013

Received: August 21, 2018.

Accepted: October 9, 2018.

Pre-published: October 11, 2018.

Correspondence: *HEINZ SILL*

heinz.sill@medunigraz.at

Supplementary Appendix

Clinical implications of subclonal *TP53* mutations in acute myeloid leukemia

Katharina T. Prochazka,[1] Gudrun Pregartner,[2] Frank Rücker,[3] Ellen Heitzer,[4] Gabriel Pabst,[1] Armin Zebisch,[1] Albert Wölfler,[1] Andrea Berghold,[2] Konstanze Döhner[3] and Heinz Sill[1]

[1]Division of Hematology, Medical University of Graz, Graz, Austria

[2]Institute for Medical Informatics, Statistics and Documentation, Medical University of Graz, Graz, Austria

[3]Department of Internal Medicine III, University Hospital of Ulm, Ulm, Germany

[4]Institute of Human Genetics, Medical University of Graz, Graz, Austria

Supplementary Methods

Details of the AMLSG studies analyzed

In trial AML-HD98A, 627 patients aged 18 to 65 years received induction therapy with idarubicine, cytarabine and etoposide (ICE). High-risk subjects were offered allogeneic hematopoietic stem cell transplantation (HSCT), intermediate-risk subjects either HSCT from a suitable related donor or, alternatively, intensive chemotherapy and low-risk subjects received intensive chemotherapy. In this study, the median age of the 596 patients with a *TP53* wild-type status was 46.8 years (range18-65) and of the 31 patients with *TP53* mutations was 57.3 years (range, 28-61), respectively. *TP53* mutated patients, thereby, represented 4.9% of the total trial cohort. Trial AMLSG 07-04 had a similar design to AML-HD98A and included 737 patients aged 18 to 61 years who were randomized to induction therapy with ICE or ICE/all-trans retinoic acid (ATRA). In this study, the median age of the 689 patients with a *TP53* wild-type status was 48.3 years (range, 18-61) and of the 48 patients with *TP53* mutations 54.1 years (range, 20-60), respectively. *TP53* mutated patients, thereby, represented 6.5% of the total trial cohort. Trial AML-HD98B included 173 patients aged 58 to 84 years who were randomized to ICE or ICE/ATRA induction with further treatment based on response. In this study, the median age of the 154 patients was 65.9 years (range, 58-85) and of the 19 patients with *TP53* mutations 66.8 years (range, 61-79), respectively. *TP53* mutated patients, thereby, represented 10.9% of the total trial cohort.

Of all patients, bone marrow (BM) and peripheral blood (PB) specimens were collected at AML diagnosis and processed by Ficoll density gradient centrifugation to enrich for mononuclear cells (*TP53* wild-type patients: BM, n=548; PB, 751; missing data, n=140. *TP53* mutated patients: BM, n=31; PB, n=49; missing data, n=18). They were then stored centrally at the biobank of the University of Ulm, Ulm, Germany.

Next generation sequencing

A total of 1537 diagnostic AML specimens were analyzed by a targeted sequencing approach with 111 genes associated with myeloid neoplasms as described previously.[1] Briefly, individual samples were indexed using a unique DNA barcode, equimolar pools of libraries were prepared and hybridized to custom RNA baits (SureSelect, Agilent) and sequenced on an Illumina HiSeq platform. Raw sequencing data were aligned to the human genome (NCBI build 37) using Burrows-Wheeler Aligner. Samples with a median overall coverage of <50x and genes with a median target coverage of <20x were excluded from

downstream analysis. Notably, the median coverage for *TP53* was 157x. Base substitutions representing the vast majority of *TP53* aberrations were identified by two parallel bioinformatics approaches (http://github.com/cancerit/CaVEMan and https://github.com/gerstung-lab/deepSNV) and annotated using the COSMIC database. Synonymous variants or germline polymorphisms at a population frequency of >1% were excluded from the study. A comparison of NGS data with pre-existing sequencing data from selected specimens generated by multiplex ligation PCR amplification or capillary sequencing showed excellent concordance rates with sensitivities of >0.9 for single base substitutions. Variant allele frequencies (VAFs) were determined by counting the number of variant reads divided by the number of reference reads. For those AML patients showing two or more *TP53* mutations, the one with the highest VAF was included into the analyses.

Serial AML specimens of one AML patient with a clonal and a subclonal *TP53* mutation obtained from the leukemia biobank at Medical University of Graz, Austria, were prepared as described previously and analyzed by ultradeep sequencing using the Safe-SeqS method.[2,3] This technology is based on molecular barcoding of individual DNA template strands to track all sequencing reads back to a single original template and correct for PCR errors during library preparation allowing detection of variant allele frequencies of <0.1%. Briefly, 10ng of DNA was amplified for 10 cycles by Phusion polymerase (Thermo Fisher) using amplicon specific primers covering *TP53, KRAS* and *FLT3* mutations whereby the sense primer contains a 12-base unique identifier (UID). After purification with Ampure XP beads (Beckman Coulter) Illumina specific adapters and indices were added in a second PCR with 35 cycles. Quality control and quantification were performed on an Agilent Bioanalyzer DNA 7500 chip (Agilent Technologies), sequencing was performed on an Illumina MiSeq in a 2x150 bp paired-end run. Generated reads were then grouped to read families according to the UID. A consensus sequence of each read family and a FastQ-file from this sequence were generated and aligned to the human reference genome (hg19) using Burrows-Wheeler transform and samtools. Alignments were visualized in the “Integrative Genomes Viewer” to detect variants.

References

1. Papaemmanuil E, Gerstung M, Bullinger L, et al. Genomic Classification and Prognosis in Acute Myeloid Leukemia. *N Engl J Med.* 2016;374(23):2209-2221.

2. Wolfler A, Erkeland SJ, Bodner C, et al. A functional single-nucleotide polymorphism of the G-CSF receptor gene predisposes individuals to high-risk myelodysplastic syndrome. *Blood.* 2005;**105**(9):3731-3736.

3. Kinde I, Wu J, Papadopoulos N, Kinzler KW, Vogelstein B. Detection and quantification of rare mutations with massively parallel sequencing. *Proc Natl Acad Sci U S A.* 2011;**108**(23):9530-9535.

Investigators and centers of the German-Austrian AML Study Group

Peter **Brossart**, M.D., Universitätsklinikum Bonn, Bonn Germany; Bernd **Hertenstein**, M.D., Henrike **Thomssen**, M.D., Klinikum Bremen Mitte, Bremen, Germany; Rainer **Haas**, M.D., Andrea **Kuendgen**, M.D., Universitätsklinikum Düsseldorf, Düsseldorf, Germany; Peter **Reimer**, M.D., Mohammed **Wattad**, M.D., Kliniken Essen Süd, Ev. Krankenhaus Essen Werden GmbH, Essen, Germany; Carsten **Schwaenen**, M.D., Klinikum Esslingen, Esslingen, Germany; Hans Gunter **Derigs**, M.D., Klinikum Frankfurt Höchst GmbH, Frankfurt, Germany; Michael **Lübbert**, M.D., Universitätsklinikum Freiburg, Freiburg, Germany; Alexander **Burchardt**, M.D., Matthias **Rummel**, M.D., Universitätsklinikum Giessen, Giessen, Germany; Volker **Runde**, M.D., Wilhelm Anton Hospital, Goch, Germany; Gerald **Wulf** M.D., Lorenz **Trümper** M.D., Universitätsklinikum Göttingen, Göttingen, Germany; Walter **Fiedler**, M.D., Universitätsklinikum Hamburg Eppendorf, Hamburg, Germany; Hans **Salwender**, M.D., Asklepios Klinik Altona, Hamburg, Germany; Elisabeth **Lange**, M.D., Evangelisches Krankenhaus Hamm, Hamm, Germany; Andrea **Sendler**, M.D., Klinikum Hanau, Hanau, Germany; Arnold **Ganser**, M.D., Jürgen **Krauter**, M.D., Brigitte **Schlegelberger**, M.D., Medizinische Hochschule Hannover, Hannover, Germany; Hartmut **Kirchner**, M.D., KRH Klinikum Siloah, Hannover, Germany; Uwe **Martens**, M.D., SLK Kliniken GmbH Heilbronn, Heilbronn, Germany; Michael **Pfreundschuh**, M.D., Gerhard **Held**, M.D., Universitätsklinikum des Saarlandes, Homburg, Germany; David **Nachbaur**, M.D., Günter **Gastl**, M.D., Universitätsklinikum Innsbruck, Innsbruck, Austria; Mark **Ringhoffer**, M.D., Martin **Bentz**, M.D., Städtisches Klinikum Karlsruhe GmbH, Karlsruhe, Germany; Hein A. **Horst**, M.D., Michael **Kneba**, M.D., Universitätsklinikum Schleswig Holstein–Campus Kiel, Kiel, Germany; Stephan **Kremers**, M.D., Caritas Krankenhaus Lebach, Lebach, Germany; Andreas **Petzer**, M.D., Krankenhaus der Barmherzigen Schwestern Linz, Linz, Austria; Gerhard **Heil**, M.D., Klinikum Ludenscheid, Ludenscheid, Germany; Thomas **Kindler**, M.D., Matthias **Theobald**, M.D., Universitätsklinikum Mainz, Mainz, Germany; Katharina **Götze**, M.D., Christian **Peschel**, M.D., Klinikum rechts der Isar der Technischen Universität München, München, Germany; Sabine **Struve**, M.D., Klinikum Schwabing, München, Germany; Peter **Schmidt**, M.D., Städtisches Klinikum Neunkirchen, Neunkirchen, Germany; Ali Nuri **Hunerliturkoglu**, M.D., Lukaskrankenhaus GmbH Neuss, Neuss; Germany; Claus Henning **Kohne**, M.D., Klinikum Oldenburg, Oldenburg, Germany; Axel **Matzdorff**, M.D., Caritas Klinik St. Theresia, Saarbrucken, Germany; Richard **Greil**,

M.D., Gudrun **Russ**, M.D., Universitätsklinikum der Paracelsus Medizinischen Universität Salzburg, Salzburg, Austria; Jochen **Greiner**, M.D., Diakonie Klinikum Stuttgart, Stuttgart, Germany; Heinz **Kirchen**, M.D., Krankenhaus der Barmherzigen Brüder, Trier, Germany; Hans Gernot **Biedermann**, M.D., Kreisklinik Trostberg, Trostberg, Germany; Helmut **Salih**, M.D., Lothar **Kanz**, M.D., Universitätsklinikum Tübingen, Tübingen, Germany; Hartmut **Döhner**, M.D., Konstanze **Döhner**, M.D., Richard F. **Schlenk**, M.D, Universitätsklinikum Ulm, Ulm, Germany; Wolfgang **Brugger**, M.D., Schwarzwald Baar Klinikum Villingen Schwenningen GmbH, Villingen Schwenningen, Germany; Elisabeth **Koller**, M.D., Hanuschkrankenhaus, Wien, Austria; Aruna **Raghavachar**, M.D., Helios Klinikum Wuppertal, Wuppertal, Germany.

Supplementary results

Supplementary Table 1. Depiction of a total of 108 clonal and subclonal *TP53* mutations found in 98/1537 patients with acute myeloid leukemia (AML). In 7 patients, two mutations and in 1 patient, four mutations were detected, respectively (marked in grey). Abbreviations: ID, identification; VAF, variant allele frequency; AA, amino acid.

Study	Patient ID	VAF (%)	cDNA change	AA change	Consequence	Karyotype
07-04	17	12.50	c.461G>A	p.G154D	missense	47,XY,del(5)(q15q33),+8
07-04	30	23.28	c.773A>C	p.E258A	missense	complex
07-04	32	13.74	c.817C>T	p.R273C	missense	46,XX
07-04	41	71.93	c.524G>A	p.R175H	missense	complex
07-04	76	45.69	c.869G>A	p.R290H	missense	47,XX,+10[20]/48,XX,+10,+21[2]
07-04	110	62.66	c.658T>C	p.Y220H	missense	complex
07-04	129	58.93	c.488A>G	p.Y163C	missense	complex
07-04	133	96.33	c.713G>A	p.C238Y	missense	complex
07-04	139	8.70	c.427G>A	p.V143M	missense	complex
07-04	177	89.01	c.524G>A	p.R175H	missense	complex
07-04	197	88.02	c.743G>A	p.R248Q	missense	complex
07-04	198	30.77	c.659A>G	p.Y220C	missense	complex
07-04	204	44.36	c.1024C>T	p.R342*	nonsense	complex
07-04	204	46.25	c.796G>C	p.G266R	missense	complex
07-04	214	77.72	c.743G>A	p.R248Q	missense	complex
07-04	228	94.44	c.503A>C	p.H168P	missense	complex
07-04	241	87.94	c.994-1G>A	NA	essential splice	46,XY
07-04	246	46.36	c.799C>T	p.R267W	missense	complex
07-04	251	70.95	c.817C>T	p.R273C	missense	complex
07-04	302	86.52	c.824G>A	p.C275Y	missense	complex
07-04	421	5.78	c.826G>C	p.A276P	missense	complex
07-04	421	12.84	c.743G>A	p.R248Q	missense	complex
07-04	421	13.98	c.587G>A	p.R196Q	missense	complex
07-04	421	38.55	c.395A>G	p.K132R	missense	complex
07-04	439	9.96	c.613T>G	p.Y205D	missense	no metaphases
07-04	462	84,75	c.583A>T	p.I195F	missense	complex
07-04	475	37.62	c.659A>G	p.Y220C	missense	46,XX,t(8;20;21)(q22;q13;q22)
07-04	578	71.64	c.524G>A	p.R175H	missense	complex
07-04	583	8.79	c.818G>A	p.R273H	missense	46,XY
07-04	654	13.41	c.524G>A	p.R175H	missense	46,XY
07-04	690	17.31	c.437G>A	p.W146*	nonsense	no metaphases
07-04	705	22.86	c.524G>A	p.R175H	missense	complex
07-04	705	20.55	c.673-1G>A	NA	essential splice	complex
07-04	743	36.62	c.493C>T	p.Q165*	nonsense	complex
07-04	873	76.99	c.524G>A	p.R175H	missense	no metaphases
07-04	890	69.66	c.527G>T	p.C176F	missense	complex
07-04	909	4.66	c.667C>T	p.P223S	missense	46,XY
07-04	911	26.96	c.832C>T	p.P278S	missense	46,XY,t(11;17)(q23;q12)[9]/ 46,XY[7]

07-04	913	5.15	c.761T>A	p.I254N	missense	no material
07-04	944	88.00	c.517G>T	p.V173L	missense	complex
07-04	954	47.22	c.742C>T	p.R248W	missense	complex
07-04	975	28.92	c.524G>A	p.R175H	missense	no metaphases
07-04	1015	83.79	c.743G>A	p.R248Q	missense	complex
07-04	1056	7.69	c.722C>T	p.S241F	missense	complex
07-04	1096	89.47	c.817C>T	p.R273C	missense	complex
07-04	1100	22.48	c.734G>A	p.G245D	missense	complex
07-04	1107	52.38	c.1154delT	p.F385fs*37	deletion_frameshift	46,XX,del(5)(q22q33),-7,+mar[20]
07-04	1120	12.24	c.388C>G	p.L130V	missense	complex
07-04	1135	33.15	c.659A>G	p.Y220C	missense	complex
07-04	1156	94.53	c.710T>A	p.M237K	missense	complex
07-04	1169	11.03	c.645T>G	p.S215R	missense	complex
07-04	1171	77.72	c.743G>A	p.R248Q	missense	complex
07-04	1216	49.47	c.584T>A	p.I195N	missense	complex
98A	28	54.37	c.400T>A	p.F134I	missense	complex
98A	69	67.95	c.701A>G	p.Y234C	missense	complex
98A	152	25.23	c.1022_1023insT	p.R342fs*5	insertion_frameshift	complex
98A	213	94.06	c.743G>A	p.R248Q	missense	complex
98A	233	53.28	c.760A>G	p.I254V	missense	no metaphases
98A	266	58.82	c.490A>G	p.K164E	missense	complex
98A	296	44.19	c.419C>A	p.T140N	missense	46,XY
98A	320	52.61	c.31G>A	p.E11K	missense	no data
98A	409	14.85	c.814G>A	p.V272M	missense	complex
98A	434	33.85	c.823T>C	p.C275R	missense	complex
98A	477	37.85	c.818G>A	p.R273H	missense	complex
98A	498	7.20	c.722C>T	p.S241F	missense	no metaphases
98A	536	96.77	c.488A>G	p.Y163C	missense	complex
98A	551	25.48	c.800G>C	p.R267P	missense	complex
98A	554	84.35	c.722C>T	p.S241F	missense	complex
98A	568	90.91	c.794T>C	p.L265P	missense	complex
98A	598	34.38	c.814G>A	p.V272M	missense	no metaphases
98A	624	73.65	c.711G>A	p.M237I	missense	complex
98A	630	96.97	c.159G>A	p.W53*	nonsense	complex
98A	661	71.74	c.439delG	p.V147fs*23	deletion_frameshift	complex
98A	691	48.00	c.848G>A	p.R283H	missense	46,XY,t(9;11)(p22;q23)[10]/47,XY,+8,t(9;11)(p22;q23)[5]
98A	692	72.28	c.722C>T	p.S241F	missense	complex
98A	695	69.83	c.722C>A	p.S241Y	missense	complex
98A	739	89.19	c.376-1G>A	NA	essential splice	complex
98A	799	64.37	c.742C>T	p.R248W	missense	complex
98A	839	79.38	c.711G>A	p.M237I	missense	complex
98A	840	91.49	c.493C>T	p.Q165*	nonsense	no metaphases
98A	870	31.78	c.608T>A	p.V203E	missense	complex
98A	919	16.94	c.160T>C	p.F54L	missense	46,XX
98A	941	78.13	c.376-2A>G	NA	essential splice	no metaphases
98A	1076	76.67	c.395A>G	p.K132R	missense	complex

98B	35	28.98	c.725G>C	p.C242S	missense	no metaphases
98B	49	87.21	c.637C>T	p.R213*	nonsense	complex
98B	69	15.71	c.25A>G	p.S9G	missense	47,XX,+11
98B	71	84.08	c.154C>T	p.Q52*	nonsense	complex
98B	87	69.93	c.577C>A	p.H193N	missense	no metaphases
98B	98	15.51	c.711G>A	p.M237I	missense	complex
98B	98	16.23	c.490A>G	p.K164E	missense	complex
98B	103	89.86	c.993+1G>A	NA	essential splice	no metaphases
98B	126	43.67	c.785G>T	p.G262V	missense	46,XY
98B	126	47.57	c.553_559+2delAGCGATGgt	p.?	deletion	46,XY
98B	199	26.99	c.645T>G	p.S215R	missense	complex
98B	199	19.44	c.560-1G>A	NA	essential splice	complex
98B	201	16.67	c.472delC	p.R158fs*12	deletion_ frameshift	complex
98B	201	18.97	c.320_321insA	p.Y107fs*1	insertion_ frameshift	complex
98B	220	57.03	c.715A>G	p.N239D	missense	complex
98B	226	81.20	c.818G>A	p.R273H	missense	47,XX,del(5)(q13q33),+6[13]/ 46,XX,del(5)(q13q33)[5]
98B	275	34.88	c.329G>T	p.R110L	missense	complex
98B	292	64.20	c.659A>G	p.Y220C	missense	46,XY,del(5)(q13q33)[10]/ 47,XY,+8[3]/46,XY[11]
98B	332	58.54	c.388C>G	p.L130V	missense	complex
98B	352	72.05	c.659A>G	p.Y220C	missense	complex
98B	352	7.69	c.438G>A	p.W146*	nonsense	complex
98B	358	76.00	c.817C>T	p.R273C	missense	complex
98B	408	77.17	c.743G>A	p.R248Q	missense	complex
98B	458	54.10	c.734G>A	p.G245D	missense	complex

Supplementary Figure 1. AML patients achieving complete remission following intensive induction therapy stratified by their *TP53* status as well as mutant *TP53* variant allele frequencies (VAFs). There is a significant difference between *TP53* wild-type patients and each of the *TP53* mutant groups (P<0.001), but not within the different VAF groups.

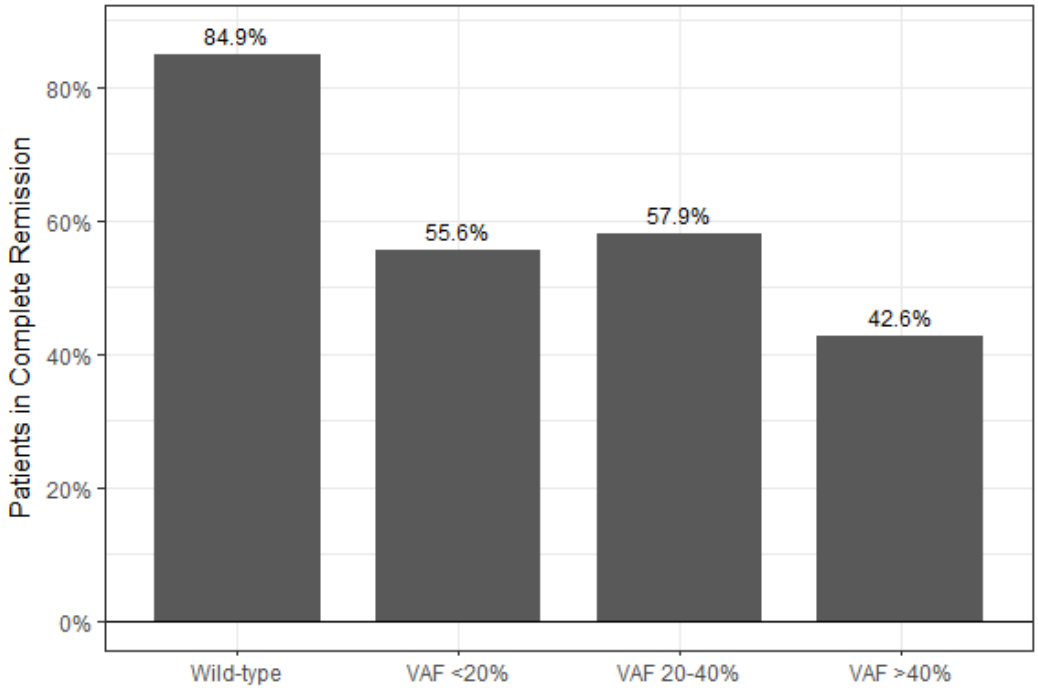

Supplementary Table 2. Three-year overall survival (OS) and median OS times including 95% confidence intervals (95% CI) of the AML cohort studied stratified by their *TP53* status as well as mutant *TP53* variant allele frequencies (VAFs).

	3-year OS (%)		**median OS (months)**	
	estimate	95% CI	estimate	95% CI
TP53 wild-type	49.1	46.5-51.8	33.6	28.4- 45.0
TP53 mutant	8.3	4.3-16.2	6.5	5.0-8.2
VAF <20%	--	--	6.9	3.9-11.7
VAF 20%-40%	5.3	0.8-35.5	6.9	5.0-17.5
VAF >40%	11.5	5.7-23.0	5.8	3.9-9.1
Total	46.5	44.0-49.1	28.1	24.3-33.5

Supplementary Table 3. Three-year event-free survival (EFS) and median EFS times including 95% confidence intervals (95% CI) of the AML cohort studied stratified by their *TP53* status as well as mutant *TP53* variant allele frequencies (VAFs).

	3-year EFS (%)		median EFS (months)	
	estimate	95% CI	estimate	95% CI
TP53 wild-type	38.3	35.9-40.9	16.5	15.0-18.2
TP53 mutant	6.3	2.9-13.6	5.7	4.3-7.4
VAF <20%	--	--	6.5	2.9-8.0
VAF 20%-40%	--	--	6.9	4.5-12.4
VAF >40%	9.8	4. -21.0	5.2	3.7-7.9
Total	36.3	33.9-38.8	15.0	13.6-16.5

Supplementary Table 4. Univariable and multivariable Cox regression analysis for event-free survival (EFS). Abbreviations: HR, hazard ratio; CI, confidence interval; VAF, variant allele frequency.

	Univariable			Multivariable		
	HR	95% CI	p-value	HR	95% CI	p-value
TP53			<0.001			<0.001
wild-type	1			1		
VAF <20%	4.18	2.58 - 6.77		3.57	2.04 - 6.26	
VAF 20%-40%	3.43	2.17 - 5.42		2.27	1.35 - 3.80	
VAF >40%	3.03	2.32 - 3.96		1.89	1.38 - 2.59	
Age	1.03	1.02 - 1.03	<0.001	1.03	1.02 - 1.03	<0.001
White blood cell count (log)	1.10	1.05 - 1.14	<0.001	1.17	1.12 - 1.22	<0.001
Cytogenetic risk			<0.001			<0.001
high	1			1		
intermediate	0.50	0.43 - 0.58		0.53	0.45 - 0.63	
low	0.28	0.22 - 0.36		0.36	0.28 - 0.47	
Type of AML			0.005			0.081
de novo	1			1		
secondary	1.56	1.17 - 2.07		1.42	1.06 - 1.91	
therapy-related	1.20	0.90 - 1.59		1.01	0.74 - 1.37	

Supplementary Table 5. Longitudinal molecular analysis of bone marrow specimens of a patient with secondary AML (sAML) and a clonal and subclonal *TP53* mutation. Variant allele frequencies (VAFs) are given for the *TP53* as well as cooperating mutations. Further abbreviations: MDS, myelodysplastic syndrome; PD, progressive disease.

Mutation	**VAF**		
	MDS	sAML	PD
TP53^{R273H}	42.3%	40.4%	64.2%
TP53^{Q104X}	0.4%	5.0%	18.6%
FLT3^{D835Y}	19.4%	31.7%	16.7%
KRAS^{Q61H}	0.0%	0.8%	25.7%